Applied Catalysis B: Environmental 303 (2022) 120928

Contents lists available at ScienceDirect

Applied Catalysis B: Environmental

journal homepage: www.elsevier.com/locate/apcatb

NH_3-SCR catalysts for heavy-duty diesel vehicles: Preparation of CHA-type zeolites with low-cost templates

Estefanía Bello [a], Pau Ferri [a], Mathias Nero [b], Tom Willhammar [b], Isabel Millet [a], Frank W. Schütze [c], Leen van Tendeloo [d], Peter N.R. Vennestrøm [e], Mercedes Boronat [a,*], Avelino Corma [a,*], Manuel Moliner [a,*]

[a] Instituto de Tecnología Química, Universitat Politècnica de València-Consejo Superior de Investigaciones Científicas, Avenida de los Naranjos s/n, 46022 València, Spain
[b] Department of Materials and Environmental Chemistry, Stockholm University, SE-106 91 Stockholm, Sweden
[c] Umicore AG & Co. KG, Hanau 63456, Germany
[d] Umicore N.V., Watertorenstraat 33, 2250 Olen, Belgium
[e] Umicore Denmark ApS, Kogle Allé 1, 2970 Hørsholm, Denmark

ARTICLE INFO

Keywords:
Selective catalytic reduction (SCR)
Nitrogen oxides (NOx)
Small pore zeolites
Chabazite (CHA)
Host-guest organic-inorganic interactions

ABSTRACT

Computer-assistance allows selecting the most adequate low-cost organic structure directing agents (OSDAs) for the crystallization of Al-rich CHA-type zeolites. The host-guest stabilization energies of tetraethylammonium (TEA), methyltriethylammonium (MTEA) and dimethyldiethylammonium (DMDEA), in combination with Na, were first theoretically evaluated. This "ab-initio" analysis reveals that two TEA show a serious steric hindrance in a *cha* cavity, whereas two MTEA would present excellent host-guest confinements. The synthesis of Al-rich CHA-type zeolites has been accomplished using TEA and MTEA. Electron diffraction and high-resolution transmission electron microscopy reveal large CHA-domains with narrow faulted GME-domains in the CHA-type material synthesized with TEA, confirming the better OSDA-directing roles of MTEA cations towards the *cha* cavity, in good agreement with DFT calculations. Cu-exchanged Al-rich CHA-type samples achieved with MTEA and TEA show excellent catalytic activity and hydrothermal stability for the selective catalytic reduction (SCR) of NOx with ammonia under conditions relevant for future heavy duty diesel conditions.

1. Introduction

Cu-containing small pore zeolites as catalysts for the selective catalytic reduction (SCR) of NOx with NH_3 have been extensively studied in the last decade [1–3], and, as a result, two small pore zeolites, CHA and AEI [4–7], have been commercialized to mitigate NOx emissions from diesel vehicles. Recent efforts focus on improving the synthesis routes of these small-pore zeolites with the aim of minimizing manufacture costs while maintaining, or even increasing, the performance of the existing materials. In this sense, one-pot synthesis routes using Cu-complexes [8–11], solvent-free or OSDA-free synthesis procedures [12,13], and different organic molecules as OSDA have been proposed to reduce the costs of the zeolites [14–17]. Since the discovery of Cu-CHA as a very active and highly stable catalyst for the SCR of NOx [5], a remarkable variety of different, more simple and less expensive OSDA molecules have been proposed as an alternative to the former OSDA N,N,N-trimethyladamantammonium (TMAda) cation [18,19]. Among them, benzyltrimethylammonium (BzTMA) [14,20], N-ethyl-N,N-dimethylcyclohexanaminium (EMCyHA) [12,15], choline (Cho) [16,21], or tetraethylammonium (TEA) [17], are probably the most representative examples allowing the crystallization of high-silica CHA zeolites with relatively high Si/Al molar ratios (above 8). It is worth noting that among the different physicochemical properties of small pore zeolites for SCR applications, their preparation with relatively high Si/Al molar ratios has been required by the automotive industry to provide high hydrothermal stability to perform under the severe conditions required due to the high temperatures achieved during particulate filter regeneration.

However, it has been recently described that Cu-containing Al-rich small pore zeolites with Si/Al ~ 4–6 [22–24], show enhanced low-temperature SCR activity compared to their high-silica counterparts, which is an important challenge under cold-start conditions [25].

* Corresponding authors.
E-mail addresses: boronat@itq.upv.es (M. Boronat), acorma@itq.upv.es (A. Corma), mmoliner@itq.upv.es (M. Moliner).

https://doi.org/10.1016/j.apcatb.2021.120928
Received 8 October 2021; Received in revised form 9 November 2021; Accepted 10 November 2021
Available online 16 November 2021

With recent regulations pushing for electrification of passenger vehicles towards and beyond 2030 more attention is focused on developing efficient NH_3-SCR catalysts for heavy-duty diesel vehicles, i.e. trucks, with different exhaust systems compared to passenger vehicles. In general, lower temperature requirements can be expected for the exhaust treatment system either due to an improved conversion of the fuel into mechanical energy or from different particulate filer regeneration strategies. For such systems the use of NH_3-SCR catalysts with lower hydrothermal stability can be applied and allow for the use of more Al-rich small pore zeolites [22]. Another relevant aspect in heavy-duty diesel vehicles is that the catalyst volume and amount is much larger compared to light-duty diesel vehicles. Thus, the overall cost of the zeolite based SCR-catalyst is even more critical, and development of less cost-intensive zeolite preparation procedures has become a clear target trying to fulfill the future needs of the automotive industry.

Herein, we describe a computer-aided methodology to select the most adequate low-cost OSDA molecule to maximize the Al-rich CHA zeolite crystallization. In a first step, a DFT study has been carried out to evaluate the ability of slightly different simple and commercially-available alkylammonium cations to stabilize the CHA structure and, among them, methyltriethylammonium (MTEA) is proposed as the preferred candidate. Then, the synthesis of Al-rich CHA-type zeolites has been attempted using TEA, MTEA and dimethydiethylammonium (DMDEA). In agreement with the theoretical information both TEA and MTEA allow the crystallization of CHA, but TEA produces less pure crystals with stacking intergrowths, as revealed by electron diffraction and high-resolution transmission electron microscopy (HRTEM). Finally, the NH_3-SCR catalytic performance for NOx abatement of the Cu-containing CHA-type materials prepared with TEA and MTEA has been evaluated under fresh and aged conditions (600 °C in steam), both presenting excellent catalytic activity and hydrothermal stability for their potential application as SCR catalysts for heavy-duty diesel vehicles.

2. Experimental

2.1. DFT calculations

Periodic density functional theory (DFT) calculations were performed using the Perdew–Burke–Ernzerhof (PBE) exchange-correlation functional within the generalized gradient approach (GGA) [26,27] as implemented in the Vienna Ab-initio Simulation Package (VASP) code [28]. The valence density was expanded in a plane wave basis set with a kinetic energy cutoff of 600 eV, and the effect of the core electrons in the valence density was taken into account by means of the projected augmented wave (PAW) formalism [29]. Integration in the reciprocal space was carried out at the Γ k-point of the Brillouin zone. Dispersion corrections to the energies were evaluated using the D2 Grimme's method. [30,31]. Electronic energies were converged to 10^{-6} eV and geometries were optimized until forces on atoms were less than 0.015 eV/Å. During geometry optimizations, the positions of all atoms in the system were allowed to relax without any restriction. The chabazite structure was modeled by means of a hexagonal unit cell with relaxed lattice parameters a = 13.756 Å, b = 13.800 Å, c = 14.836 Å, α = 90.135°, β = 89.936° and γ = 120.101° containing 36 T atoms (Si or Al) and 72 O atoms. Realistic models with a Si/Al ratio of 5 were generated by replacing six framework Si atoms per unit cell by Al (locations described in the results section and SI). The negative charges were compensated by combinations of organic TEA, MTEA and DMDEA and inorganic sodium cations. Interaction energies per T atom were calculated as:

$$E_{int}/T=[E(CHA\text{-}6SDA)–E(CHA)–6E(SDA)]/36$$

where E(CHA-6SDA) is the total energy of the system with Si/Al = 5 containing six organic or inorganic (Na^+) structure directing agents (SDA), E(CHA) is the total energy of the CHA unit cell with six framework Al atoms, and E(SDA) is the total energy of the isolated organic or inorganic cations.

2.2. Zeolite synthesis

2.2.1. Zeolite synthesis using tetraethylammonium (TEA) as OSDA [sample TEA]

1.29 g of FAU zeolite (FAU, Zeolyst CBV500 with Si/Al=2.6, 80 wt% TO_2) was added to 3.15 g of a 35 wt% aqueous solution of tetraethylammonium hydroxide (Sigma-Aldrich). The mixture was stirred during 10 min for homogenization. Afterwards, 6.54 g of sodium silicate (31.1 wt% SiO_2, 6.7 wt% Na_2O, values measured by ICP) was added, and the synthesis mixture was maintained under stirring the required time to evaporate the excess of water until achieving the desired gel concentration. The final gel composition was SiO_2: 0.0625 Al_2O_3: 0.15 TEA: 0.28 NaOH: 7 H_2O. The resultant gel was charged into a stainless steel autoclave with a Teflon liner. The crystallization was then conducted at 150 °C for 1 day under dynamic conditions. The solid product was filtered, washed with abundant water, and dried at 100 °C. The solids were calcined at 580 °C for 5 h in air to remove the occluded organic molecules.

2.2.2. Zeolite synthesis using methyltriethylammonium (MTEA) as OSDA [sample MTEA]

1.29 g of FAU zeolite (FAU, Zeolyst CBV500 with Si/Al=2.6, 80 wt% TO_2) was added to 14.91 g of a 6.7 wt% aqueous solution of methyltriethylammonium hydroxide (Sigma-Aldrich). The mixture was stirred during 10 min for homogenization. Afterwards, 6.54 g of sodium silicate (31.1 wt% SiO_2, 6.7wt% Na_2O, values measured by ICP) was added, and the synthesis mixture was maintained under stirring the required time to evaporate the excess of water until achieving the desired gel concentration. The final gel composition was SiO_2: 0.0625 Al_2O_3: 0.15 MTEA: 0.28 NaOH: 7 H_2O. The resultant gel was charged into a stainless steel autoclave with a Teflon liner. The crystallization was then conducted at 150 °C for 1 day under dynamic conditions. The solid product was filtered, washed with abundant water, and dried at 100 °C. The solids were calcined at 580 °C for 5 h in air to remove the occluded organic molecules.

2.2.3. Zeolite synthesis using dimethyldiethylammonium (DMDEA) as OSDA [sample DMDEA]

1.29 g of FAU zeolite (FAU, Zeolyst CBV500 with Si/Al=2.6, 80 wt% TO_2) was added to 4.47 g of a 20 wt% aqueous solution of dimethyldiethylammonium hydroxide (Sigma-Aldrich). The mixture was stirred during 10 min for homogenization. Afterwards, 6.53 g of sodium silicate (31.1 wt% SiO_2, 6.7 wt% Na_2O, values measured by ICP) was added, and the synthesis mixture was maintained under stirring the required time to evaporate the excess of water until achieving the desired gel concentration. The final gel composition was SiO_2: 0.0625 Al_2O_3: 0.15 DMDEA: 0.28 NaOH: 7 H_2O. The resultant gel was charged into a stainless steel autoclave with a Teflon liner. The crystallization was then conducted at 150 °C for 1 day under dynamic conditions. The solid product was filtered, washed with abundant water, and dried at 100 °C. The solids were calcined at 580 °C for 5 h in air to remove the occluded organic molecules.

2.2.4. Cu-exchange treatments

The Cu ion exchange of the calcined zeolites was carried out by introducing 0.50 g zeolites in 50 mL of an aqueous solution of Cu $(CH_3COO)_2{\cdot}H_2O$ [47.2 mg of $Cu(CH_3COO)_2{\cdot}H_2O$ dissolved in 50 mL of water], maintaining a solid/liquid ratio of 10 g/L at room temperature for 10 h. Afterwards, the solids were filtered and washed with distilled water, dried and calcined at 580 °C in air for 5 h.

2.2.5. Hydrothermal ageing treatments of Cu-exchanged zeolites

The Cu-exchanged zeolites were subjected to a hydrothermal treatment at 600 °C using a 300 mL/min flow rate with 10% water, 10% of O_2 and balanced with nitrogen for 16 h.

2.3. Characterization

Powder X-ray diffraction (PXRD) measurements were performed with a multi sample Philips X'Pert diffractometer equipped with a graphite monochromator, operating at 40 kV and 35 mA, and using Cu Kα radiation (λ = 0.1542 nm).

Chemical analyses were carried out in a Varian 715-ES ICP-Optical Emission spectrometer, after solid dissolution in HNO_3/HCl/HF aqueous solution.

^{27}Al MAS NMR spectra were recorded at room temperature with a Bruker AV 400 spectrometer at 104.2 MHz with a spinning rate of 10 kHz and 9° pulse length of 0.5 μs with a 1 s repetition time. ^{27}Al chemical shift was referred to $Al^{3+}(H_2O)_6$.

The thermo-gravimetric (TG) analysis was performed with a Mettler Toledo TGA/SDATA851e between 20 and 800 °C, assigning the loss of weight up to 150 °C to adsorbed water.

The morphology of the samples was studied by field emission scanning electron microscopy (FESEM) using a ZEISS Ultra-55 microscope.

The sample was prepared for transmission electron microscopy (TEM) studies using ultra microtomy in order to obtain thin sections and to access the desired crystallographic direction for imaging. The zeolite powder was dried in oven overnight and embedded in an epoxy resin (Agar Low Viscosity Resin) which was hardened at 60 °C for 24 h. Sectioning was performed using a Leica Ultracut UCT with a 45° diamond knife from Diatome to an estimated thickness of 50 nm. After cutting, the sections were transferred to holey carbon coated copper grids. Selected area electron diffraction (SAED) patterns as well as high resolution transmission electron microscopy (HRTEM) images were collected using a JEOL JEM-2100F microscope operated at 200 kV. Structure projection reconstruction was performed based on through-focus series, each consisting of 20 HRTEM images collected with a constant focus step of 106.6 Å. The structure projection images were reconstructed using the software QFocus [32].

2.4. NH_3-SCR catalytic test

The catalytic activity was evaluated for the catalytic reduction of NOx with NH_3 in a fixed bed, quartz tubular reactor with 1.2 cm inner diameter. 40 mg sieve fractionated catalyst was used diluted in 1.2 g of silicon carbide. The catalysts were introduced in the reactor and heated up to 550 °C in a 300 mL/min flow of nitrogen and maintained at this temperature for one hour. Afterwards, the feed was admitted over the catalyst while maintaining a flow of 300 mL/min. The feed composition for the catalytic tests performed over the Cu-containing catalysts was 500 ppm NO, 550 ppm NH_3, 7%O_2 and 5% H_2O. The reaction temperature was decreased stepwise between 550 and 170 °C. The conversion of NO was measured under steady state conversion at each temperature using a CLD8xx analyzer (ECO PHYSICS).

3. Results

3.1. DFT evaluation of host-guest stabilization with simple alkylammonium cations

Different works in the literature have successfully described computer-assisted approaches to calculate the interaction energies between OSDAs and zeolite frameworks to guide their experimental preparation [33–36]. To provide fundamental knowledge for the synthesis of Al-rich CHA crystals using low-cost templates, the stabilization offered by three simple alkylammonium cations (TEA, MTEA and DMDEA see Fig. 1) within the unit cell of CHA zeolite has been

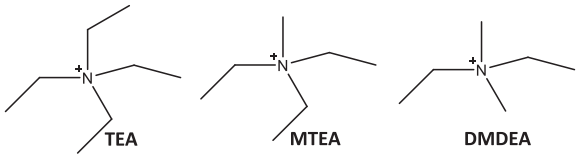

Fig. 1. Simple alkylammonium cations employed as organic structures directing agents (OSDAs) in the present study.

theoretically evaluated by means of DFT calculations, using a catalyst model with a fixed Si/Al ratio of 5. Taking into account that the unit cell of the CHA framework contains 36-T atoms and three CHA cages, a Si/Al molar ratio of 5 implies the presence of six tetrahedrally-coordinated framework Al atoms, with an average distribution of 2 Al species per CHA cage. Since the negative charges generated by the presence of Al in the framework must be compensated by organic or inorganic cations, different alternatives comprising OSDA and sodium cations have been considered, ranging from two OSDA molecules to two sodium cations per CHA cage (see Fig. S1). Moreover, it has been described recently that the Al distribution within the CHA cavities can be influenced by the organic and inorganic cations used in the synthesis [37,38]. Thus, three different Al distributions, including Al pairs in 6-rings and 8-rings, have been considered in the DFT study to evaluate if the calculated interaction energies could be influenced by the Al positioning (see Fig. S2). The first conclusion from the DFT results is that the calculated interaction energies (E_{int}/T) are not influenced by the initial Al distribution considered when using these simple alkylammonium cations, since analogous E_{int}/T values are obtained for each zeolite-cation pair with differences in the range of ± 1–2 kJ/mol (see Tables S1–S3). Thus, to simplify the interpretation of the DFT results, the E_{int}/T values obtained for the three different Al distributions have been averaged (see Fig. 2).

The host-guest stabilization energy provided by DMDEA is worse for all OSDA-Na configurations considered compared to TEA and MTEA, indicating a consistently better structure directing effect of TEA and MTEA towards Al-rich CHA across various compositions compared to DMDEA. The E_{int}/T values calculated for DMDEA remain almost constant around −70 kJ/mol for all configurations (see Fig. 2), and provides only a slightly better stabilization effect compared to the 0 + 6 configuration (E_{int}/T = −63 kJ/mol) where only sodium cations occupy the *cha* cages. In contrast, substantial differences in the calculated stabilization energies are observed for TEA and MTEA depending on the spatial distribution of the OSDA and Na cations. When considering 1 OSDA and 1 Na per *cha* cage (configuration 3 + 3B), both TEA and MTEA allow analogous E_{int}/T values (−83 KJ/mol, see Fig. 2), while for the 3 + 3 A configuration presenting the local incorporation of two OSDA molecules in the same *cha* cavity, the stabilization energy achieved with MTEA is

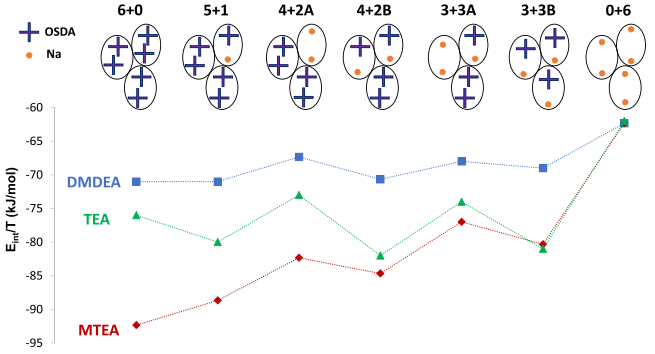

Fig. 2. Theoretical stabilization energies calculated for the different OSDA and Na configurations within the unit cell of CHA (E_{int}/T refers to the stabilization energy obtained per tetrahedral site of the zeolite and it has been calculated as the average stabilization energy of three different Al distributions along CHA cavities proposed in Fig. S1).

slightly better than with TEA (−77 and −74 kJ/mol, respectively). This effect is more pronounced as the number of OSDA molecules increases (see configurations 6 + 0, 5 + 1, 4 + 2 A and 4 + 2B in Fig. 2). Indeed, the difference in stabilization energy between TEA and MTEA is 9 kJ/mol for the distributions containing two *cha* cages occupied by a pair of OSDA molecules (4 + 2 A and 5 + 1 configurations), and further increases to 16 kJ/mol when exclusively 6 OSDA molecules are incorporated in the unit cell of CHA (2 OSDA/*cha* cavity, configuration 6 +0).

To understand this trend, the optimized geometries of the 6 + 0 and 3 + 3B configurations for TEA, MTEA and DMDEA are shown in Fig. 3. The Na cations always occupy positions close to the 6-ring plane of the small double-six-ring units (see Fig. 3a), irrespectively of the number of Al in the 6-ring, while the bulkier organic cations are around the center of the CHA cavities, with the methyl and ethyl groups oriented towards the 8-ring windows (see Fig. S3). The host-guest stabilization energy includes the electrostatic interaction between the compensating cations and the negatively charged framework, as well as Van der Waals and dispersion interactions between the hosted organic molecules and the framework oxygen atoms. The contribution of this last term depends on the geometrical fitting between the hosted OSDA molecules and the zeolite cavity, and explains the lower stabilization obtained with the smallest molecule considered, DMDEA, because it is not large enough to fill the CHA cavity. In configuration 3 + 3B (see Fig. 3a) the Na cations are close to the 6-ring plane at the top of the cage, while the three ethyl groups of TEA and MTEA interact closely with the oxygens forming the 8-ring windows at the bottom part of the cavity (see Fig. S3), leading to a similar stabilization energy. When two OSDA molecules are located within the same cavity (see for instance configuration 6 + 0 in Fig. 3b) the favorable stabilization energy of MTEA compared to TEA may indicate that TEA is sterically hindered and MTEA is geometrically just a better fit as a consequence of the single methyl-group.

To check this point, a neutral approach has been applied to exclusively evaluate the steric influence of the organic molecules within the *cha* cages without considering the electrostatic interactions. A pure silica CHA unit cell containing six neutral OSDA molecules in which N is substituted by C has been employed to calculate interaction energies (see Fig. S4 and Table S4). This simple approximation clearly shows that two TEA molecules do not fit within the CHA cavity, as revealed by the positive interaction energies obtained ($E_{int}/T = 9$ kJ/mol, see Table S4), whereas the neutral approximation of MTEA molecules within the pure silica *cha* cavity presents favorable stabilization energies ($E_{int}/T = -9$ kJ/mol, see Table S4). Thus, from an overall stabilization energy point of view, the MTEA cation seems to be a preferred simple alkylammonium candidate to facilitate the synthesis of Al-rich CHA zeolites.

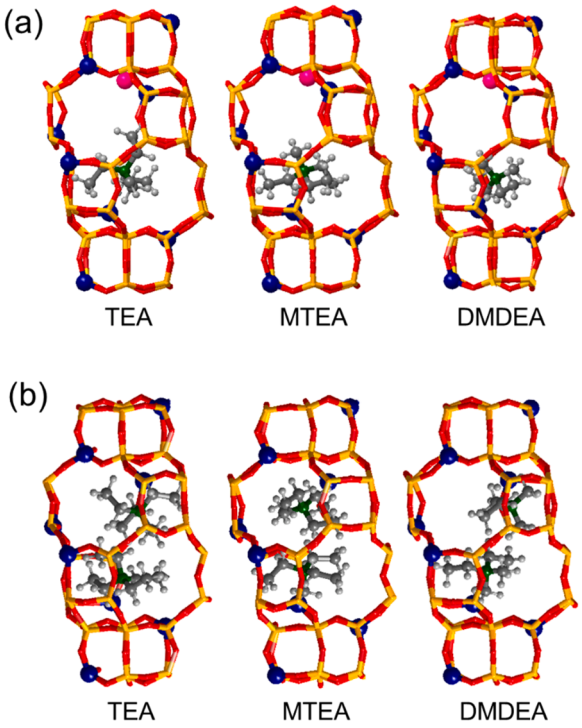

Fig. 3. Optimized geometries of TEA, MTEA and DMDEA within the CHA cage in a 3 + 3B configuration containing Na (a) or in a 6 + 0 configuration (b). Framework Si and O atoms are depicted as yellow and red sticks. Al, Na, C, N and H atoms are depicted as blue, pink, gray, green and white balls, respectively. (For interpretation of the references to color in this figure legend, the reader is referred to the web version of this article.)

3.2. Zeolite synthesis and characterization

The synthesis of Al-rich CHA zeolites was attempted using TEA, MTEA and DMDEA as OSDAs under identical molar gel compositions (see experimental section for synthesis details). A low-silica FAU was applied as the source of Al and Si together with additional Si introduced using sodium silicate.

The PXRD patterns of the resultant as-prepared solids show the main formation of the CHA structure with TEA and MTEA, whereas a very different PXRD pattern is obtained with DMDEA (see PXRD patterns of the as-prepared samples in Fig. 4a). A deeper inspection of the PXRD pattern of the sample prepared with DMDEA reveals the presence of a mixture of LEV and ESV phases (see comparison with simulated PXRD patterns in Fig. S5). Both LEV and ESV phases are also cage-based small pore zeolites with smaller cavities than CHA structure [39,40]. Although their synthesis has been preferentially described using small cyclic ammonium cations [39,40], the preparation of LEV has also been described using DMDEA as OSDA [41], suggesting that the smaller size of DMDEA would favor the formation of *lev* and *esv* cavities instead of CHA.

As the PXRD patterns of the CHA-type materials obtained with TEA and MTEA are analyzed in detail, interesting differences are observed between them (see Fig. 4). In general, some of the diffraction peaks of the solid achieved using TEA are broader and less intense than those observed in the sample synthesized with MTEA (see Fig. 4). While this feature could easily be interpreted as nanosized crystals, this is not the case. FE-SEM images clearly show that the sample synthesized with TEA are even slightly larger than the one achieved with MTEA (700 and 500 nm for the sample synthesized with TEA and MTEA, respectively, see Fig. 5). FE-SEM images also reveal that the crystals synthesized with TEA consistently show the appearance of stripes on the external surface of the crystals (see Fig. 5-left). It has been described in the literature that the presence of stacking faults can not only influence the zeolite crystal growth, but also the final surface morphology of the crystals [42]. Thus, the combination of broader peaks in the PXRD patterns of the as-prepared and calcined samples synthesized with TEA together with their different crystal surface morphology could be compatible with the formation of intergrowth zeolite systems.

In order to unravel the crystalline characteristics of the CHA-type material obtained when using TEA as OSDA, the calcined sample has been studied by HRTEM and electron diffraction. Selected area electron diffraction (SAED) pattern from the CHA-type sample synthesized with TEA shows a combination of sharp reflections and diffusely scattered lines along the c^*-axis (see Fig. S6a). The strongest intensities in the diffraction pattern can be indexed by two CHA lattices viewed along [100] related by a mirror plane perpendicular to the c^*-axis (see Fig. S6b), while the diffusely scattered tails in between the reflections are consistent with a small domain size of the layered disorder (see Fig. S6a). HRTEM image shows a layered disorder in good agreement with the observations from electron diffraction (see Fig. 6a). Interestingly, a line profile along the stacking direction reveals a layer thickness of 4.6 Å (see Fig. S7) which is consistent with the thickness of a double layer of 6 rings in the ABC-6 family of zeolites. This fact is true also in the

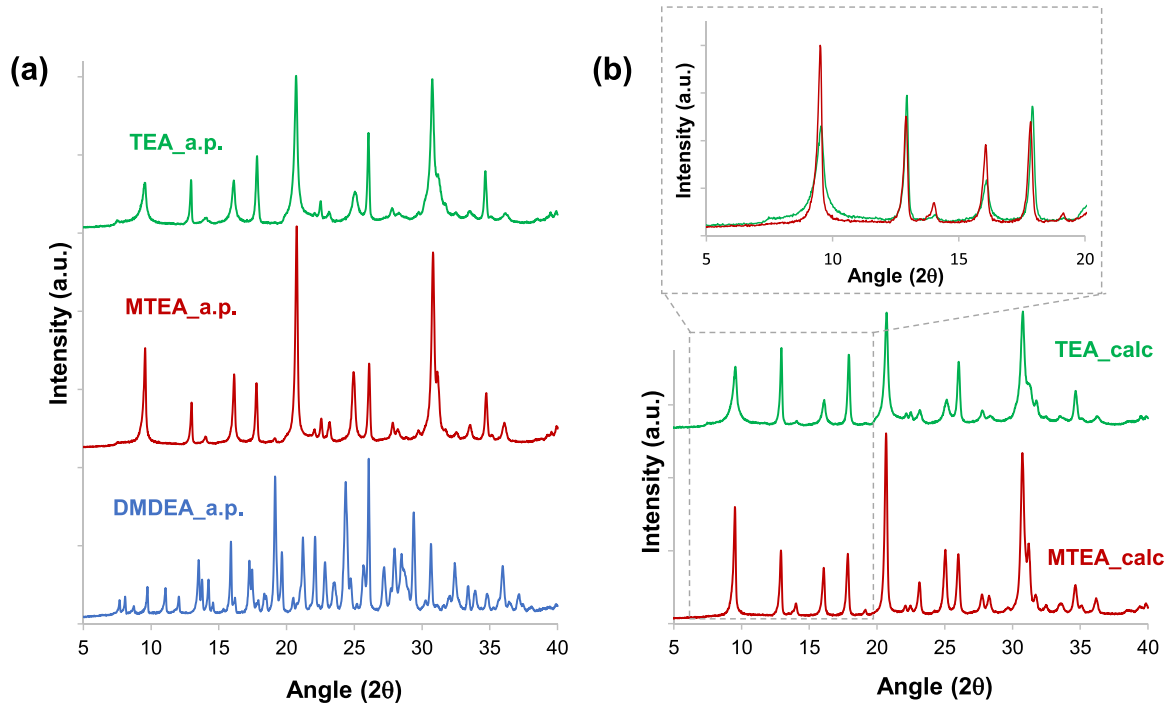

Fig. 4. PXRD patterns of the as-prepared materials (a) and after being calcined in air at 580 °C (b).

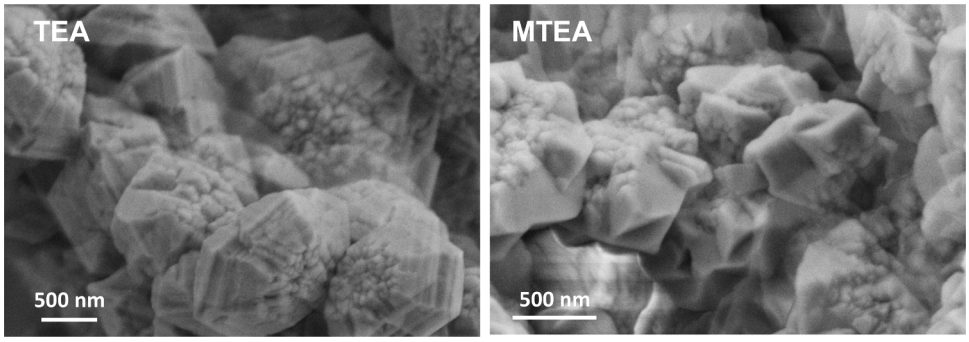

Fig. 5. FE-SEM images of the CHA-type zeolites achieved using TEA and TMEA.

domain across twin boundaries, which means that the structure is entirely built from layers of double 6-rings. The material contains domains of CHA with AABBCCAA type stacking, twinning to AACCBBAA stacking (see straight red lines in Fig. 6a and structure model in Fig. 6b). The twinning creates a GME-like stacking (AABBAA) locally at the very twin boundary, as reflected in the position of the kink of the red line in Fig. 6b, but, from the HRTEM study, it can be stated that there are no apparent extended regions of GME-type stacking. However, the twin boundary itself locally alters the structure and creates a different cage (see cage highlighted in green in Fig. 6b), which is larger than *cha* cage (see Fig. 7). This experimental observation for the Al-rich CHA-type zeolite synthesized with TEA is in good agreement with DFT analysis, where local concentration of two TEA molecules could have steric hindrance within the *cha* cage, facilitating the formation of larger cages within the zeolite crystals when using TEA as compared to MTEA.

The chemical composition of the as-prepared CHA-type materials has been evaluated by ICP analysis, presenting both materials analogous Si/Al molar ratios (~ 4.6–4.9, see Table 1) and comparable Na contents (~ 4.0 wt%, see Table 1). ^{27}Al MAS NMR spectra of the two CHA-type zeolites synthesized with MTEA and TEA clearly reveal the exclusive presence of the Al species in tetrahedral coordination (see signal centered at ~ 56 ppm in Fig. 8). Combining ICP and ^{27}Al MAS NMR spectra with the fact that the unit cell of CHA contains three *cha* cavities and 36 T-atoms, the average presence of ~ 2–2.2 aluminum species and ~ 1.1–1.3 sodium cations per *cha* cavity can be estimated for these two CHA-type materials (see Table 2).

In addition, the two as-prepared Al-rich CHA-type materials synthesized with TEA and MTEA have also been characterized by elemental and thermogravimetric analyses to quantify the organic molecules trapped per *cha* cavity during the hydrothermal synthesis. The overall weight losses measured for the CHA-type materials synthesized with TEA and MTEA were 17.2% and 15.7 wt%, respectively, presenting both a very similar weight loss between 200 and 700 °C (~ 10.1–10.5 wt%, see Table 1). Elemental analysis shows a slightly higher organic content in the CHA-type sample prepared with MTEA (1.5 wt% N and 8.3 wt% C, see Table 1) than TEA (1.2 wt% N and 8.0 wt% C, see Table 1). Combining the thermogravimetric analysis with the elemental analysis, it is possible to estimate that the average number of OSDA molecules per cavity approaches ~ 1 OSDA per *cha* cavity, being 0.9 and 0.8 for MTEA and TEA, respectively (see Table 2). It is worth noting that the structure of CHA as pure phase has been considered for these OSDA estimations for both samples.

Chemical and elemental analyses certainly indicate that the most probable configuration along the Al-rich CHA-type materials

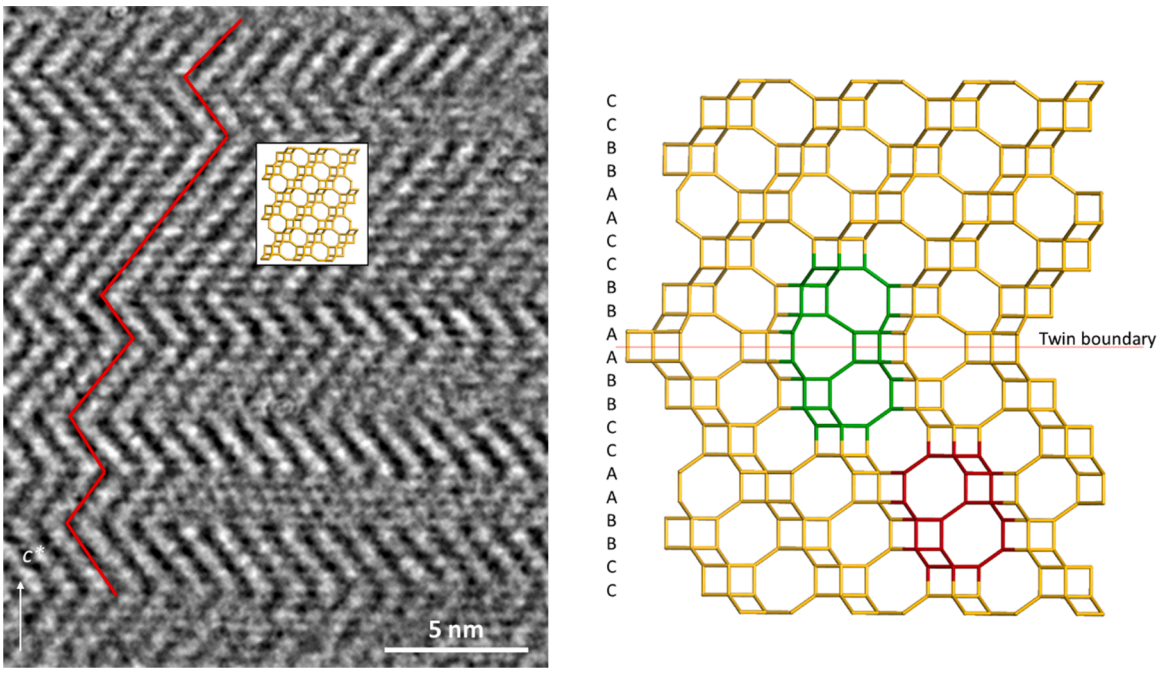

Fig. 6. (a) HRTEM image acquired along the [100] direction of the CHA-type zeolite synthesized with TEA. Twinning in small domains is present as indicated by the red guideline. CHA structure is shown as inset for reference. (b) Structure model for the twin boundary in the structure of CHA with the larger cage (in green) created around the twin boundary. A CHA cage is shown in red. Oxygen atoms are omitted for clarity in the structure models. (For interpretation of the references to color in this figure legend, the reader is referred to the web version of this article.)

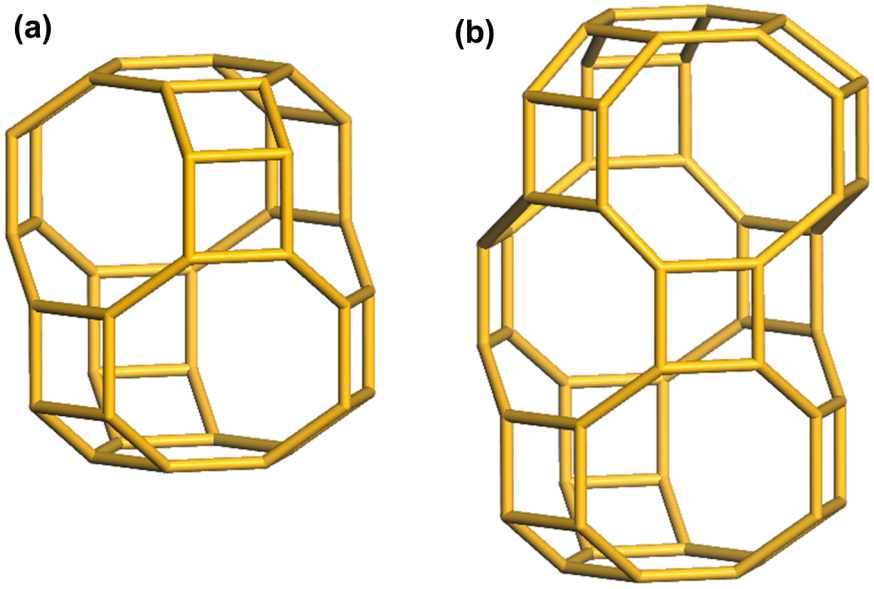

Fig. 7. Structure models for CHA cage (a) and for the cage present at the CHA twin-boundary (b). Oxygen atoms are omitted in the structure models for clarity.

Table 1
Physico-chemical properties of the CHA-type zeolites synthesized using TEA and MTEA as OSDAs in their as-prepared forms and after being calcined and Cu-exchanged.

	ICP analysis			Elemental analysis			TGA analysis		
Sample	Si/Al	Na (wt%)	Cu (wt%)	N (wt%)	C (wt%)	C/N	< 200 °C (wt%)	200–700 °C (wt%)	Total (wt%)
TEA_a.p.	4.6	4.1	–	1.24	7.98	7.5	6.2	10.0	16.2
MTEA_a.p.	4.9	3.6	–	1.49	8.31	6.5	5.6	10.1	15.7
Cu-TEA	4.4	1.7	3.9	–	–	–	–	–	–
Cu-MTEA	4.7	1.2	4.1	–	–	–	–	–	–

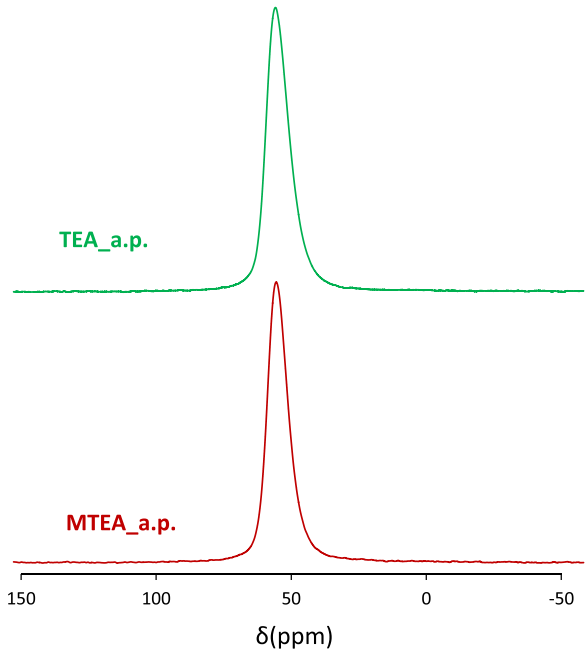

Fig. 8. ^{27}Al MAS NMR spectra of the as-prepared Al-rich CHA-type materials synthesized with MTEA and TEA.

Table 2
Quantification of the number of Al, Na and OSDA species per CHA cavity.

Sample	Al/Cav	Na/Cav	OSDA/Cav
TEA_a.p.	2.2	1.3	0.8
MTEA_a.p.	2.0	1.1	0.9

synthesized using the low-cost TEA and MTEA organic molecules would be the 3 + 3B model (see Fig. S2), where the CHA cages would be filled by 1 OSDA molecule and 1 Na cation. As seen in Fig. 2, the stabilization energies for the 3 + 3B model using TEA and MTEA are very similar, explaining the excellent ability of both OSDAs to direct the crystallization of CHA. Despite the 3 + 3B model is the most reasonable conformation along the bulk CHA-type crystals, small local changes on the OSDA and sodium concentrations during the nucleation/crystallization processes, could facilitate the appearance of local OSDA-rich or Na-rich areas. In these cases, some of the less stable host-guest configurations for a particular OSDA, such as for instance the 4 + 2 A or 3 + 3 A conformations with two OSDA molecules in the same cavity (see Fig. 2) could be accessible, maybe explaining the CHA/GME intergrowth with the formation of cavities larger than *cha* cages when employing TEA molecule as OSDA.

3.3. Catalytic evaluation of Al-rich CHA-type catalysts for the SCR of NOx

Copper was exchanged in the calcined zeolite materials synthesized with TEA and MTEA (see experimental section for details), to evaluate their catalytic performance in the NH_3-SCR reaction. The amount of copper in the final catalysts was similar (~3.9% and 4.1 wt% for the Cu-containing CHA-type zeolite prepared with TEA and MTEA, respectively, see Table 1).

The two fresh Cu-containing CHA-type samples show very similar NO conversion profiles when tested at different reaction temperatures for the NH_3-SCR of NO reaction (see experimental section for details and Fig. 9). Both Cu-CHA catalysts show almost entire NO conversion values in a broad temperature range (between 250 and 500 °C, see Cu-MTEA and Cu-TEA in Fig. 9), and, interestingly, they also present good low-temperature NO conversions below 250 °C (X_{NO}~55% at 170 °C, see Fig. 9). As comparative purposes, other high-silica Cu-CHA-type materials tested under the same reaction conditions always present X_{NO} below 35% [11,17], demonstrating the great benefits for low-temperature NOx conversion of the Al-rich CHA-type materials presented here.

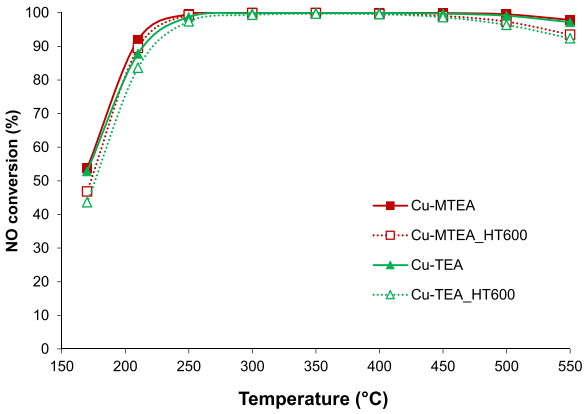

Fig. 9. NH_3-SCR of NOx activity of Cu-containing CHA-type catalysts prepared using TEA and MTEA as OSDAs in their fresh form and after being aged in steam at 600 °C for 16 h. Reaction conditions: 500 ppm of NO, 550 ppm of NH_3, and 7% of O_2, 5% of H_2O, with a gas hourly space velocity of 450,000 mL/h g_{cat}.

These Cu-CHA-type materials have also been aged at 600 °C with steam for 16 h, conditions that can be considered adequate to evaluate the long-term stability of Cu-based zeolites for heavy-duty diesel vehicles. Very interestingly, the two aged Cu-containing CHA-type materials maintain most of their NH_3-SCR performance compared to their fresh counterparts, including low- and high-temperature behavior (see Cu-MTEA_HT600 and Cu-TEA_HT600 in Fig. 9).

These preliminary catalytic results highlight the similar catalytic performance of both Al-rich CHA-type materials prepared with low-cost and simple OSDAs for NH_3-SCR of NOx in heavy-duty applications, even when a significant stacking intergrowth is present in the CHA-type catalyst prepared with TEA. Thus, one could speculate that the copper stabilization along the Al-rich *cha* cavities and along the new larger cavities present in the twin boundaries (see Fig. 6b) would be similar. Moreover, it is worth noting that these Al-rich CHA-type zeolites show an excellent NH_3-SCR performance in their fresh and aged forms, even when a significant amount of sodium cations remain in the final catalysts after Cu-exchange treatments (above 1 wt% in both materials, see Table 1). What we have shown is that Al-rich CHA-type zeolites can not only be synthesized with low-cost OSDA molecules, but furthermore, these materials do not require additional successive cation exchange treatments to remove alkali cations providing more simplicity and flexibility when addressing future automotive zeolites.

4. Conclusions

Aiming to select the most adequate low-cost OSDA molecule to maximize the Al-rich CHA zeolite crystallization, a number of simple and commercially-available alkylammonium cations with slight differences on their alkyl chain groups, as tetraethylammonium (TEA), methyltriethylammonium (MTEA) and dimethyldiethylammonium (DMDEA) have been considered in this study. In a first step, the host-guest stabilization energies provided by different combinations of organic and inorganic (Na) cations within the CHA structure have been evaluated by means of DFT calculations. Remarkably better stabilization energies are obtained for TEA and MTEA as compared to DMDEA, due to a better interaction of the ethyl groups with the 8-ring windows of CHA. Moreover, when varying the OSDA and Na distribution along the CHA unit cell, it is found that the local incorporation of two TEA molecules in

a single *cha* cavity is limited by steric hindrance, while two MTEA molecules present an improved host-guest confinement.

Based on this "ab-initio" theoretical results, the preparation of Al-rich CHA-type zeolites has been attempted using TEA, MTEA and DMDEA. The crystallization of CHA-type crystals are exclusively achieved with TEA and MTEA, while a mixture of ESV and LEV crystals are accomplished with DMDEA. However, some differences between the CHA-type materials obtained with TEA and MTEA are observed when comparing their powder X-ray diffraction (PXRD) patterns and crystal morphologies by scanning electron microscopy (SEM). Electron diffraction as well as high-resolution transmission electron microscopy (HRTEM) clearly reveal the presence of crystals with stacking intergrowths in the case of the Al-rich CHA-type material synthesized with TEA, formed by large domains of CHA with narrow faulted GME domains that allows the presence of larger cavities than *cha* cages. These experimental observations are in good agreement with theoretical calculations, and expose the importance of selecting the proper OSDA molecule to design target zeolites, where differences as small as one methyl group between the organic molecules can severely influence zeolite crystallization.

Finally, the two Al-rich CHA-type materials prepared with TEA and MTEA have been exchanged with copper and their catalytic performance in the NH_3-SCR reaction has been evaluated under fresh and hydrothermal aging conditions relevant for future heavy duty diesel conditions. Both materials exhibit similar and excellent catalytic activity and hydrothermal stability, unaffected by the presence of sodium cations or the presence of stacking intergrowths in the samples synthesized using TEA as OSDA.

CRediT authorship contribution statement

All the authors have contributed to the design of experiments, the acquisition and analysis of the experimental data and the writing of the manuscript.

Declaration of Competing Interest

The authors declare that they have no known competing financial interests or personal relationships that could have appeared to influence the work reported in this paper.

Acknowledgments

This work has been supported by Umicore and by the Spanish Government-MCIU through RTI2018-101033-B-I00 (MCIU/AEI/FEDER, UE) and PID2020-112590GB-C21 (AEI/FEDER, UE). T.W. acknowledges financial support by the Swedish Research Council (Grant No. 2019-05465). E.B. acknowledges the Spanish Government-MCIU for a FPI scholarship (PRE2019-088360). P.F. thanks ITQ for a contract. The Electron Microscopy Service of the UPV is acknowledged for their help in sample characterization. The computations were performed on the Tirant III cluster of the Servei d'Informàtica of the University of Valencia.

Appendix A. Supplementary material

Supplementary data associated with this article can be found in the online version at doi:10.1016/j.apcatb.2021.120928.

References

[1] D.W. Fickel, E. D'Addio, J.A. Lauterbach, R.F. Lobo, The ammonia selective catalytic reduction activity of copper-exchanged small-pore zeolites, Appl. Catal. B Environ. 102 (3–4) (2011) 441–448, https://doi.org/10.1016/j.apcatb.2010.12.022.

[2] A.M. Beale, F. Gao, I. Lezcano-Gonzalez, C.H.F. Peden, J. Szanyi, Recent advances in automotive catalysis for NOx emission control by small-pore microporous materials, Chem. Soc. Rev. 44 (20) (2015) 7371–7405, https://doi.org/10.1039/C5CS00108K.

[3] M. Moliner, C. Martínez, A. Corma, Synthesis strategies for preparing useful small pore zeolites and zeotypes for gas separations and catalysis, Chem. Mater. 26 (1) (2014) 246–258, https://doi.org/10.1021/cm4015095.

[4] J.H. Kwak, R.G. Tonkyn, D.H. Kim, J. Szanyi, C.H.F. Peden, Excellent activity and selectivity of Cu-SSZ-13 in the selective catalytic reduction of NOx with NH3, J. Catal. 275 (2) (2010) 187–190, https://doi.org/10.1016/j.jcat.2010.07.031.

[5] I. Bull, W.M. Xue, P. Burk, R.S. Boorse, W.M. Jaglowski, G.S. Koermer, A. Moini, J. A. Patchett, J.C. Dettling, M.T. Caudle, Copper CHA Zeolite Catalysts, US7601662, 2009.

[6] M. Moliner-Marin, C. Franch-Martí, A.E. Palomares-Gimeno, A. Corma-Canós, P.N. R. Vennesstrom, A. Kustov, J.R. Thogersen, Method and System for the Purification of Exhaust Gas from an Internal Combustion Engine, WO2013159825, 2013.

[7] M. Moliner, C. Franch, E. Palomares, M. Grill, A. Corma, Cu–SSZ-39, an active and hydrothermally stable catalyst for the selective catalytic reduction of NOx, Chem. Commun. 48 (66) (2012) 8264, https://doi.org/10.1039/c2cc33992g.

[8] L. Ren, L. Zhu, C. Yang, Y. Chen, Q. Sun, H. Zhang, C. Li, F. Nawaz, X. Meng, F.-S. Xiao, Designed copper–amine complex as an efficient template for one-pot synthesis of Cu-SSZ-13 zeolite with excellent activity for selective catalytic reduction of NOx by NH3, Chem. Commun. 47 (35) (2011) 9789, https://doi.org/10.1039/c1cc12469b.

[9] L. Xie, F. Liu, L. Ren, X. Shi, F.-S. Xiao, H. He, Excellent performance of one-pot synthesized Cu-SSZ-13 catalyst for the selective catalytic reduction of NOx with NH3, Environ. Sci. Technol. 48 (1) (2014) 566–572, https://doi.org/10.1021/es4032002.

[10] U. Deka, I. Lezcano-Gonzalez, S.J. Warrender, A. Lorena Picone, P.A. Wright, B. M. Weckhuysen, A.M. Beale, Changing active sites in Cu–CHA catalysts: DeNOx selectivity as a function of the preparation method, Microporous Mesoporous Mater. 166 (2013) 144–152, https://doi.org/10.1016/j.micromeso.2012.04.056.

[11] R. Martínez-Franco, M. Moliner, J.R. Thogersen, A. Corma, Efficient one-pot preparation of Cu-SSZ-13 materials using cooperative OSDAs for their catalytic application in the SCR of NOx, ChemCatChem 5 (11) (2013) 3316–3323, https://doi.org/10.1002/cctc.201300141.

[12] X. Wang, Q. Wu, C. Chen, S. Pan, W. Zhang, X. Meng, S. Maurer, M. Feyen, U. Müller, F.-S. Xiao, Atom-economical synthesis of a high silica CHA zeolite using a solvent-free route, Chem. Commun. 51 (95) (2015) 16920–16923, https://doi.org/10.1039/C5CC05980A.

[13] Y. Wang, T. Nishitoba, Y. Wang, X. Meng, F.-S. Xiao, W. Zhang, B. Marler, H. Gies, D. Vos, De, U. Kolb, M. Feyen, R. McGuire, A.-N. Parvulescu, U. Müller, T. Yokoi, Cu-exchanged CHA-type zeolite from organic template-free synthesis: an effective catalyst for NH3–SCR, Ind. Eng. Chem. Res. 59 (2020) 7375–7382, https://doi.org/10.1021/acs.iecr.9b06708.

[14] S.I. Zones, Preparation of Molecular Sieves Using a Structure Directing Agent and An N, N, N-Triakyl Benzyl Quaternary Ammonium Cation, US20080075656, 2008.

[15] G. Cao, M.M. Mertens, K.G. Strohmaier, R.B. Hall, T.H. Colle, M. Afeworki, A.J. Bons, W.J. Mortier, C. Kliewer, H. Li, A.S. Guram, R.J. Saxton, M.T. Muraoka, J.C. Yoder, Chabazite-Containing Molecular Sieve, Its Synthesis and Its Use in the Conversion of Oxygenates to Olefins, US7094389B2, 2006.

[16] B. Chen, R. Xu, R. Zhang, N. Liu, Economical way to synthesize SSZ-13 with abundant ion-exchanged Cu+ for an extraordinary performance in selective catalytic reduction (SCR) of NOx by ammonia, Environ. Sci. Technol. 48 (23) (2014) 13909–13916, https://doi.org/10.1021/es503707c.

[17] N. Martín, M. Moliner, A. Corma, High yield synthesis of high-silica chabazite by combining the role of zeolite precursors and tetraethylammonium: SCR of NOx, Chem. Commun. 51 (49) (2015) 9965–9968, https://doi.org/10.1039/C5CC02670A.

[18] S.I. Zones, Zeolite SSZ-13 and Its Method of Preparation, US4544538, 1985.

[19] S.I. Zones, Conversion of faujasites to high-silica chabazite SSZ-13 in the presence of N,N,N-Trimethyl-1-adamantammonium iodide, J. Chem. Soc. Faraday Trans. 87 (22) (1991) 3709, https://doi.org/10.1039/ft9918703709.

[20] S.I. Zones, Translating new materials discoveries in zeolite research to commercial manufacture, Microporous Mesoporous Mater. 144 (1–3) (2011) 1–8, https://doi.org/10.1016/j.micromeso.2011.03.039.

[21] X. Wang, R. Zhang, H. Wang, Y. Wei, Strategy on effective synthesis of SSZ-13 zeolite aiming at outstanding performances for NH3-SCR process, Catal. Surv. Asia 24 (2) (2020) 143–155, https://doi.org/10.1007/s10563-020-09300-w.

[22] Y. Shan, W. Shan, X. Shi, J. Du, Y. Yu, H. He, A comparative study of the activity and hydrothermal stability of Al-rich Cu-SSZ-39 and Cu-SSZ-13, Appl. Catal. B Environ. 264 (2020), 118511, https://doi.org/10.1016/j.apcatb.2019.118511.

[23] C. Paolucci, A.A. Parekh, I. Khurana, J.R. Di Iorio, H. Li, J.D. Albarracin Caballero, A.J. Shih, T. Anggara, W.N. Delgass, J.T. Miller, F.H. Ribeiro, R. Gounder, W. F. Schneider, Catalysis in a cage: condition-dependent speciation and dynamics of exchanged Cu cations in SSZ-13 zeolites, J. Am. Chem. Soc. 138 (18) (2016) 6028–6048, https://doi.org/10.1021/jacs.6b02651.

[24] Z. Zhao, R. Yu, C. Shi, H. Gies, F.-S. Xiao, D. De Vos, T. Yokoi, X. Bao, U. Kolb, R. McGuire, A.-N. Parvulescu, S. Maurer, U. Müller, W. Zhang, Rare-earth ion exchanged Cu-SSZ-13 zeolite from organotemplate-free synthesis with enhanced hydrothermal stability in NH3-SCR of NOx, Catal. Sci. Technol. 9 (1) (2019) 241–251, https://doi.org/10.1039/C8CY02033G.

[25] F. Gao, J. Szanyi, On the hydrothermal stability of Cu/SSZ-13 SCR catalysts, Appl. Catal. A Gen. 560 (2018) 185–194, https://doi.org/10.1016/j.apcata.2018.04.040.

[26] J.P. Perdew, K. Burke, M. Ernzerhof, Generalized gradient approximation made simple, Phys. Rev. Lett. 77 (18) (1996) 3865–3868, https://doi.org/10.1103/PhysRevLett.77.3865.

[27] J.P. Perdew, K. Burke, M. Ernzerhof, Generalized gradient approximation made simple, Phys. Rev. Lett. 78 (7) (1997) 1396, https://doi.org/10.1103/PhysRevLett.78.1396 [Phys. Rev. Lett. 77, 3865 (1996)].
[28] G. Kresse, J. Furthmüller, Efficient iterative schemes for ab initio total-energy calculations using a plane-wave basis set, Phys. Rev. B 54 (16) (1996) 11169–11186, https://doi.org/10.1103/PhysRevB.54.11169.
[29] P.E. Blöchl, Projector augmented-wave method, Phys. Rev. B 50 (24) (1994) 17953–17979, https://doi.org/10.1103/PhysRevB.50.17953.
[30] S. Grimme, Accurate description of van Der Waals complexes by density functional theory including empirical corrections, J. Comput. Chem. 25 (12) (2004) 1463–1473, https://doi.org/10.1002/jcc.20078.
[31] S. Grimme, J. Antony, S. Ehrlich, H. Krieg, A consistent and accurate ab initio parametrization of density functional dispersion correction (DFT-D) for the 94 elements H-Pu, J. Chem. Phys. 132 (15) (2010), 154104, https://doi.org/10.1063/1.3382344.
[32] W. Wan, S. Hovmöller, X. Zou, Structure projection reconstruction from through-focus series of high-resolution transmission electron microscopy images, Ultramicroscopy 115 (2012) 50–60, https://doi.org/10.1016/j.ultramic.2012.01.013.
[33] M. Moliner, P. Serna, Á. Cantín, G. Sastre, M.J. Díaz-Cabanas, A. Corma, Synthesis of the Ti-silicate form of BEC polymorph of β-zeolite assisted by molecular modeling, J. Phys. Chem. C 112 (49) (2008) 19547–19554, https://doi.org/10.1021/jp805400u.
[34] S.K. Brand, J.E. Schmidt, M.W. Deem, F. Daeyaert, Y. Ma, O. Terasaki, M. Orazov, M.E. Davis, Enantiomerically enriched, polycrystalline molecular sieves, Proc. Natl. Acad. Sci. 114 (20) (2017) 5101–5106, https://doi.org/10.1073/pnas.1704638114.
[35] X. Hong, W. Chen, G. Zhang, Q. Wu, C. Lei, Q. Zhu, X. Meng, S. Han, A. Zheng, Y. Ma, A.-N. Parvulescu, U. Muller, W. Zhang, T. Yokoi, X. Bao, B. Marler, D.E. Vos, U. De; Kolb, F.-S. Xiao, Direct synthesis of aluminosilicate IWR zeolite from a strong interaction between zeolite framework and organic template, J. Am. Chem. Soc. 141 (2019) 18318–18324, https://doi.org/10.1021/jacs.9b09903.
[36] D. Schwalbe-Koda, S. Kwon, C. Paris, E. Bello-Jurado, Z. Jensen, E. Olivetti, T. Willhammar, A. Corma, Y. Román-Leshkov, M. Moliner, R. Gómez-Bombarelli, A priori control of zeolite phase competition and intergrowth with high-throughput simulations, Science 374 (6565) (2021) 308–315, https://doi.org/10.1126/science.abh3350.
[37] J.R. Di Iorio, R. Gounder, Controlling the isolation and pairing of aluminum in chabazite zeolites using mixtures of organic and inorganic structure-directing agents, Chem. Mater. 28 (7) (2016) 2236–2247, https://doi.org/10.1021/acs.chemmater.6b00181.
[38] E.M. Gallego, C. Li, C. Paris, N. Martín, J. Martínez-Triguero, M. Boronat, M. Moliner, A. Corma, Making nanosized CHA zeolites with controlled Al distribution for optimizing methanol-to-olefin performance, Chem. Eur. J. 24 (55) (2018) 14631–14635, https://doi.org/10.1002/chem.201803637.
[39] B.J. Campbell, A.K. Cheetham, G. Bellussi, L. Carluccio, G. Perego, R. Millini, D. E. Cox, The synthesis of the new zeolite, ERS-7, and the determination of its structure by simulated annealing and synchrotron X-ray powder diffraction, Chem. Commun. No. 16 (1998) 1725–1726, https://doi.org/10.1039/a803572e.
[40] C.V. Tuoto, J.B. Nagy, A. Nastro, Synthesis and characterization of levyne type zeolite obtained from gels with different SiO2/Al2O3 ratios, Stud. Surf. Sci. Catal. 105 (1997) 213–220, https://doi.org/10.1016/S0167-2991(97)80558-7.
[41] K. Yamamoto, T. Ikeda, M. Onodera, A. Muramatsu, F. Mizukami, Y. Wang, H. Gies, Synthesis and structure analysis of RUB-50, an LEV-type aluminosilicate zeolite, Microporous Mesoporous Mater. 128 (1–3) (2010) 150–157, https://doi.org/10.1016/j.micromeso.2009.08.016.
[42] N.S. John, S.M. Stevens, O. Terasaki, M.W. Anderson, Evolution of surface morphology with introduction of stacking faults in zeolites, Chem. Eur. J. 16 (7) (2010) 2220–2230, https://doi.org/10.1002/chem.200902101.